Radical Ligands

DOI: 10.1002/anie.201005953

Hidden Noninnocence: Theoretical and Experimental Evidence for Redox Activity of a β-Diketiminate(1−) Ligand**

Marat M. Khusniyarov, Eckhard Bill, Thomas Weyhermüller, Eberhard Bothe, and Karl Wieghardt**

The properties and coordination chemistry of β-diketiminates, so-called NacNac⁻ ligands, are well established.[1] This ligand system has been studied extensively during the last decade, and it has found widespread use as a versatile auxiliary ligand whose steric parameters and electronic properties can be readily adjusted to fine-tune the properties of a coordinated metal ion. Recently NacNac⁻ ligands have been used to stabilize low-valent metal ions, as well as metal ions with low coordination numbers (<4).[2,3] Although metal complexes with NacNac⁻ ligands have been shown to participate in exciting redox reactions,[3,4] no evidence for involvement of the ligand in redox events has been reported. On the other hand, it is now well recognized that redox-active ligands acting as "electron buffers" can play a crucial role in catalysis.[5] Here we demonstrate that the monoanionic NacNac⁻ ligand, which is a closed-shell ligand, undergoes one-electron oxidation to form a neutral ligand π radical NacNac• when coordinated to a Ni^{II} ion. Note that the intraligand bond lengths of a common redox-active ligand strongly depend on its oxidation state and can thus be determined by high-resolution X-ray crystallography in most cases.[6] However, we show that the oxidation state of a NacNac ligand has only a minor influence on the intraligand bond lengths, and may therefore be difficult to detect by X-ray crystallography. This renders the NacNac ligand system fundamentally different from known chelating redox-active ligands.[7]

The parent neutral complex **1** (Scheme 1) was prepared according to a literature procedure.[8] Here we report its molecular structure and redox properties, as well as a reinvestigation[8,9] of its electronic structure. X-ray crystallography reveals a twisted tetrahedral geometry of **1** with a twist angle α between the two nearly planar NCCCN chelators of 72.3° (Figure 1).[10] The two pairs of *N*-CH_3 groups apparently prevent formation of a square-planar geometry around the Ni^{II} ion. The Ni–N distances of 1.949(1) Å point to a high-spin

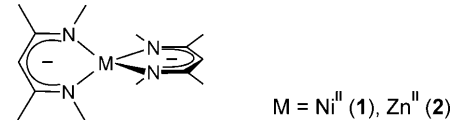

M = Ni^{II} (**1**), Zn^{II} (**2**)

Scheme 1. Metal complexes of this work.

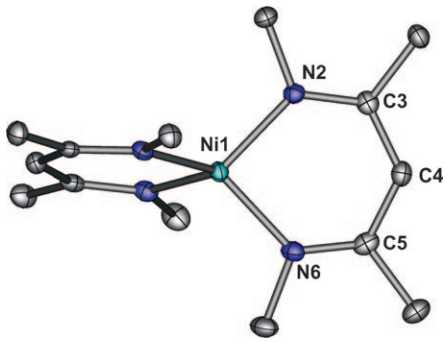

Figure 1. Molecular structure of **1** (site symmetry D_2), with thermal ellipsoids drawn at 50% probability (Ni cyan, N blue, C gray).

state of the metal ion ($S=1$). The high-spin state is corroborated by magnetic susceptibility measurements, whereby an effective magnetic moment of 2.78 μ_B was measured on a microcrystalline sample at room temperature (Figure S1, Supporting Information). Thus, **1** is a classical Werner-type complex featuring two closed-shell monoanionic NacNac⁻ ligands coordinated to a high-spin Ni^{II} center.[8,9]

Cyclic voltammograms of **1** measured in CH_2Cl_2 solution at room temperature reveal one reversible oxidation wave centered at −0.33 V versus Fc^+/Fc and a second irreversible oxidation at about 0.44 V (Figure S2, Supporting Information). Coulometric measurements at low temperatures establish that the first oxidation is a one-electron process. The electrochemically generated $\mathbf{1}^+$ species is not stable at room temperature, and we have been unable to isolate salts of $\mathbf{1}^+$ generated by chemical methods. Nevertheless, we were able to investigate the electronic structure of $\mathbf{1}^+$ generated electrochemically at −25 °C. The oxidation $\mathbf{1}\rightarrow\mathbf{1}^+$ is accom-

[*] Dr. M. M. Khusniyarov, Dr. E. Bill, Dr. T. Weyhermüller, Dr. E. Bothe, Prof. Dr. K. Wieghardt
Max Planck Institut für Bioanorganische Chemie
Stiftstrasse 34–36, 45470 Mülheim an der Ruhr (Germany)
Fax: (+49) 208-306-3951
E-mail: wieghardt@mpi-muelheim.mpg.de
Homepage:
http://ewww.mpi-muelheim.mpg.de/bac/index_en.php
Dr. M. M. Khusniyarov
Department of Chemistry and Pharmacy
Friedrich-Alexander-University Erlangen-Nürnberg
Egerlandstr. 1, 91058 Erlangen (Germany)
Fax: (+49) 9131-85-27367
E-mail: marat.khusniyarov@chemie.uni-erlangen.de
Homepage: http://www.chemie.uni-erlangen.de/khusniyarov

[**] M.M.K. is grateful to the Max Planck Society and Fonds der Chemischen Industrie for fellowships.

Supporting information for this article is available on the WWW under http://dx.doi.org/10.1002/anie.201005953.

panied by a color change from light orange to intense blue, appearance of a strong MLCT band at 591 nm, and a broad ligand-to-ligand intervalence charge-transfer band in the NIR region (Figure 2, see Supporting Information for assignment).

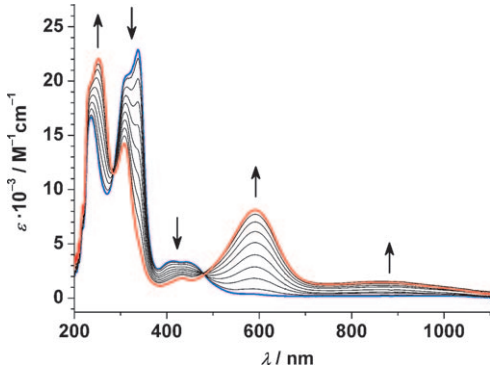

Figure 2. UV/Vis/NIR spectroelectrochemical response of the transition $\mathbf{1}\rightarrow\mathbf{1}^+$ measured in CH_2Cl_2 at −25 °C (0.1 M $[n\mathrm{Bu_4N}]PF_6$).

The EPR spectrum of $\mathbf{1}^+$ measured in frozen MeCN solution shows a rhombic signal with $g_1 = 2.25$, $g_2 = 2.09$, and $g_3 = 2.03$ (Figure S3, Supporting Information). The large anisotropy of the g tensor ($\Delta g = 0.22$), position of the signals near $g_e = 2.00$, and the absence of a half-field signal can only be ascribed to a doublet ground state ($S = 1/2$) of $\mathbf{1}^+$ with spin density predominantly located at the metal center.

Although the crystal structure of $\mathbf{1}^+$ is not available, its molecular structure is expected to be similar to the twisted tetrahedral geometry of parent complex **1**, as the two pairs of bulky *N*-CH_3 groups are expected to prevent formation of a square-planar complex. Indeed, known four-coordinate metal complexes featuring two CH_3–N···N–CH_3 chelators show variation of the corresponding dihedral angle from 62 to 84°.[11] Furthermore, DFT calculations corroborate a twisted tetrahedral geometry of $\mathbf{1}^+$ ($\alpha = 78°$, vide infra).

If the oxidation $\mathbf{1}\rightarrow\mathbf{1}^+$ is a metal-centered process, then the oxidation state of the nickel ion would be +3, with a d^7 electronic configuration. On the basis of ligand-field theory, a d^7 ion in a tetrahedral ligand environment is expected to be a high-spin ion with $S = 3/2$, as three unpaired electrons occupy the t_2 set of d orbitals. The twist towards square-planar geometry splits the t_2 set and ultimately results in spin pairing and switching to a low-spin ground state in a truly square-planar complex. The calculated geometry of $\mathbf{1}^+$ ($\alpha = 78°$) is much closer to a tetrahedral case ($\alpha = 90°$) than to a square-planar scenario ($\alpha = 0°$) and points to a high-spin state of a hypothetical Ni^{III} ion in $\mathbf{1}^+$. More importantly, the isoelectronic Co^{II} ion remains in a high-spin state in some closely related twisted tetrahedral complexes even when the twist angle drops to 54°.[12] Thus, the assumed metal-based oxidation $\mathbf{1}\rightarrow\mathbf{1}^+$ must result in formation of a high-spin Ni^{III} species ($S = 3/2$). However, this is in contradiction with EPR spectroscopy, which unambiguously shows the presence of an $S = 1/2$ species.

The only reasonable explanation for the doublet ground state of $\mathbf{1}^+$ is that the one-electron oxidation $\mathbf{1}\rightarrow\mathbf{1}^+$ is a ligand-centered process. If this is the case, an open-shell ligand NacNac$^\bullet$ ($S_L = 1/2$) is expected to be strongly antiferromagnetically coupled to a high-spin Ni^{II} ion ($S_{Ni} = 1$) to give an overall doublet ground state ($S_t = 1/2$).[13] Indeed, the EPR spectrum measured for $\mathbf{1}^+$ closely resembles those of some other high-spin Ni^{II} complexes containing one antiferromagnetically coupled ligand π radical.[13] Thus, $\mathbf{1}^+$ must contain a high-spin Ni^{II} ion chelated by one radical ligand NacNac$^\bullet$.

The oxidation states of the nickel ion and the ligands in **1** and $\mathbf{1}^+$ were further assigned on the basis of DFT calculations. The B3LYP-optimized structure of **1** is in good agreement with the X-ray structure (Table 1). According to the analysis

Table 1: Experimental and calculated (spin-unrestricted B3LYP-DFT) bond lengths [Å] and twist angles α[a] [°].

	1 (X-ray)[b]	**1**	$\mathbf{1}^+$	**2** (X-ray)[b]	**2**	$\mathbf{2}^+$	$\mathbf{2}^{2+}$
M–N	1.949(1)	1.976	1.941	1.958(1)	2.016	2.012	2.028
C–N[c]	1.325(2)	1.330	1.329	1.204(1)	1.329	1.324	1.316
C–C[c]	1.409(2)	1.413	1.415	1.438(1)	1.416	1.427	1.447
α	72	90	78	81	90	90	90

[a] Dihedral angle between two planes of the ligand NCCCN backbones. [b] Averaged values. [c] Bonds of the ligand NCCCN backbone.

of reduced orbital populations[14] the electronic configuration of the Ni ion is $(d_{x^2-y^2})^2(d_{z^2})^2(d_{xz})^2(d_{yz})^1(d_{xy})^1$, that is, high-spin Ni^{II} (Table S1, Supporting Information).[15] The four Ni–N bonds are strongly covalent; thus, spin populations of both d_{yz} and d_{xy} orbitals are each 0.76, significantly less than the theoretical value of 1.00. An important result is that the atomic (total) spin density at nickel in **1** is only +1.58, and +0.42 spins are transferred from the metal ion to the ligands through covalency.

The doublet state ($S = 1/2$) calculated for $\mathbf{1}^+$ is energetically lower than the quartet state ($S = 3/2$) by 30 kJ mol^{-1}, that is, in agreement with the results obtained from EPR spectroscopy. The calculated Ni–N distances of $\mathbf{1}^+$ ($S = 1/2$) are on average 0.035 Å shorter than those of **1**, whereas intraligand bond lengths are essentially identical in the two complexes. Spin populations of Ni d_{yz} and d_{xy} orbitals drop further and reach 0.69 and 0.54, respectively, leaving a spin of +1.38 at the metal ion, whereas a spin of −0.38 is delocalized over two ligands (Table S1, Supporting Information). As we have pointed out previously,[14] the electronic configuration and the physical oxidation state[6,16] of the metal center in a complex lose their meaning when the fractional spin densities of the metal d orbitals approach a value of 0.50, as observed here. However, if we compare the spin density distributions in **1** and $\mathbf{1}^+$ (Table 2), it becomes clear that for the oxidation $\mathbf{1}\rightarrow$

Table 2: Comparison of spin densities for **1** and $\mathbf{1}^+$ (spin-unrestricted B3LYP-DFT, Löwdin populations).

	Ni_{total}	d_{xy}	Ligands
$\mathbf{1}^+$ ($S = 1/2$)	1.38	0.54	−0.38
1 ($S = 1$)	1.58	0.76	0.42
difference	−0.20	−0.22	−0.80

$\mathbf{1}^+$, corresponding to the total loss of one spin ($S=1\rightarrow S=1/2$), only a fraction of 0.20 of a spin is removed from the Ni center, whereas 0.80 is removed from the ligands. Hence, the oxidation $\mathbf{1}\rightarrow\mathbf{1}^+$ is predominantly a ligand-centered process and the oxidation state of the Ni ion remains +2.

Note that highly covalent metal–ligand bonding is responsible for the remarkably low spin densities at the metal ion for both **1** and $\mathbf{1}^+$. Contraction of Ni–N bonds by oxidation can be ascribed to some degree to partial metal oxidation, but predominantly it arises from enhanced π backdonation to the oxidized form of the ligand. Surprisingly, the intraligand bond lengths do not change significantly with changing oxidation state of the NacNac ligand. This is a consequence of the particular nature of the redox-active ligand orbital (vide infra) and of valence delocalization. The latter can be inferred from the spin density plot for $\mathbf{1}^+$, which shows negative spin density equally delocalized over both ligands (Figure 3). The metal d_{xy} orbital is strongly antiferromagnetically coupled to a ligand-based MO of π character (Figure 4). Both the calculated orbital overlap for two magnetic orbitals of $S_{ab}=0.69$, which is significantly less than 1.0, and the expectation value of the total spin-squared operator $\mathbf{S}^2$ of 1.29, which is significantly larger than 0.75, confirm the validity of the broken-symmetry solution and the presence of a ligand radical.[17]

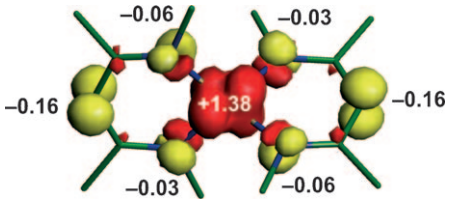

Figure 3. Broken-symmetry spin density map for $\mathbf{1}^+$.

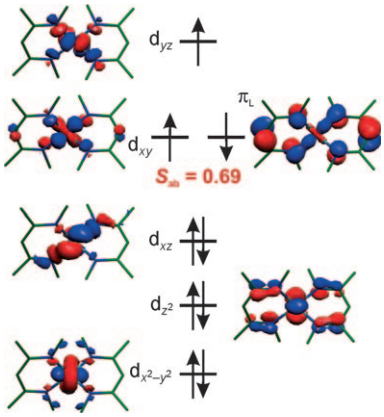

Figure 4. Qualitative MO scheme for $\mathbf{1}^+$.

To further examine the NacNac-centered oxidation observed for **1**, we synthesized zinc analogue **2**, which cannot undergo metal-based oxidation. The molecular structure of **2** is similar to that of **1** and shows a twisted tetrahedral geometry ($\alpha=81°$, Figure S4 of the Supporting Information). The cyclic voltammogram of **2** also features two oxidative waves (Figures S5 and S6, Supporting Information). The first oxidation is shifted by about 0.25 V towards more positive potentials compared to **1** when measured at 200 $mV\,s^{-1}$ scan rate. Its irreversibility indicates that the Zn^{II} ion is not able to readily stabilize the NacNac$^{\bullet}$ radical. This is probably due to the higher effective charge of the Zn^{II} ion, which results in lower energies of the Zn d orbitals and, consequently, less metal–ligand covalency in **2**. Density functional calculations confirm the ligand-centered nature of the one-electron and two-electron oxidations of **2**. The spin density for $\mathbf{2}^+$ is delocalized over both NacNac ligands and is negligible at the Zn^{II} ion (Figure S7, Supporting Information). Spin density at both NacNac ligands is doubled upon the second oxidation generating $\mathbf{2}^{2+}$ (calculated as a spin triplet, Figure S8 of the Supporting Information).

Note that the redox-active MO of the NacNac ligand is a nonbonding π orbital that has two nodes at the imine carbon atoms (Figure 5). Consequently, variations of its occupation are not expected to change intraligand bond lengths significantly. Thus, oxidation $\mathbf{2}\rightarrow\mathbf{2}^+$ yields $[Zn^{II}(NacNac^-)(NacNac^{\bullet})]^+$, which contains one closed-shell $NacNac^-$ anion and one open-shell NacNac$^{\bullet}$ π radical, whereby the ligand spin is delocalized over both ligands. This leads to shortening of C–N bonds by only 0.005 A and elongation of C–C bonds of NCCCN fragment by 0.011 Å (Table 1). The second oxidation to $[Zn^{II}(NacNac^{\bullet})_2]^{2+}$ is accompanied by shortening of the C–N bonds by 0.013 Å (relative to parent **2**) and elongation of C–C bonds by 0.030 Å. Such small changes would be difficult to detect by X-ray crystallography. These observations indicate that the NacNac ligands are fundamentally different from the well-investigated α-diimine derivatives and their oxygen and sulfur analogues, all of which show a significant dependence of the intraligand bond lengths on the oxidation state of the ligand. Thus, the noninnocence of the NacNac ligand seems to be hidden from X-ray crystallography.

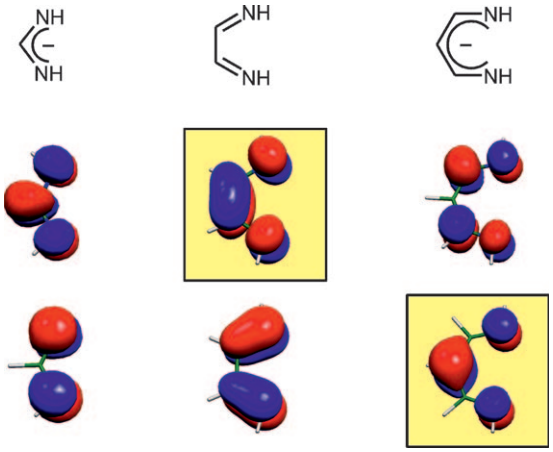

Figure 5. Frontier π orbitals of aldiminate$^-$ (left), α-diimine (center), and $NacNac^-$ (right). Occupied MOs are shown at the bottom, and unoccupied orbitals at the top; established redox-active MOs are enclosed in squares.

Since NacNac ligands bearing bulky aromatic substituents are more commonly used than those with alkyl groups as in **1**, it is noteworthy that the former can be oxidized to neutral ligand radicals too. However, the presence of electron-withdrawing substituents or substituents that are less electron donating than a methyl group is expected to shift the oxidation potential of a NacNac ligand towards more positive potentials. Due to the form of the redox-active orbital of a NacNac ligand, the oxidation potential will be more sensitive towards substituents at the 1-, 3-, and 5-positions of the ligand.

More generally, on the basis of the form and symmetry of the π orbitals (Figure 5), we propose that for any bidentate ligand with an even number of atoms in the π system (e.g., diimines, NCCN; $n=4$) the intraligand bond lengths will depend strongly on the oxidation state of the ligand. Therefore, in most cases the oxidation state of such a ligand can be determined by high-resolution X-ray crystallography.[6,18] In contrast, for a ligand with an odd number of atoms in the ligand backbone (e.g., NacNac, NCCCN; $n=5$), the oxidation state of the ligand has only a minor influence on the intraligand bond length, which may therefore be difficult to detect by X-ray crystallography.

Experimental Section

1 was prepared according to a known procedure starting from a doubly protonated form $(H_2L)(BF_4)$ of the ligand (L: 1,2,4,5-tetramethyl-NacNac).[8]

2: $ZnCl_2$ (273 mg, 2 mmol), $(H_2L)(BF_4)$ (856 mg, 4 mmol), and NaO*t*Bu (865 mg, 9 mmol) were stirred at room temperature in dry MeOH (12 mL) for 21 h. The slightly colored solution was decanted and the white solid was extracted with toluene (8 mL). After the volume of toluene solution was decreased crystalline white **2** was obtained. Yield: 433 mg (69%). Elemental analysis calcd (%) for $C_{14}H_{26}N_4Zn$: C 53.25, H 8.3, N 17.7; found: C 53.0, H 8.3, N 17.6. ^{1}H NMR (400 MHz, CD_2Cl_2, 20 °C, TMS): $\delta=1.89$ (s, 12 H, CH_3), 2.90 (s, 12 H, CH_3), 4.27 ppm (s, 2 H, CH); ^{13}C NMR (101 MHz, CD_2Cl_2, 20 °C, TMS): $\delta=21.2$ (CH_3), 37.6 (CH_3), 92.0 (CH), 168.1 ppm (C=N); EI-MS: *m*/*z* (%): 314 (57) [M^+], 299 (14), 284 (20), 189 (21), 123 (100).

Received: September 22, 2010
Published online: January 7, 2011

Keywords: chelates · density functional calculations · nickel · N ligands · redox chemistry

[1] a) D. J. Mindiola, *Angew. Chem.* **2009**, *121*, 6314; *Angew. Chem. Int. Ed.* **2009**, *48*, 6198; b) C. J. Cramer, W. B. Tolman, *Acc. Chem. Res.* **2007**, *40*, 601; c) H. W. Roesky, S. Singh, V. Jancik, V. Chandrasekhar, *Acc. Chem. Res.* **2004**, *37*, 969; d) L. Bourget-Merle, M. F. Lappert, J. R. Severn, *Chem. Rev.* **2002**, *102*, 3031.

[2] a) D. J. Mindiola, *Acc. Chem. Res.* **2006**, *39*, 813; b) J. Spielmann, D. Piesik, B. Wittkamp, G. Jansen, S. Harder, *Chem. Commun.* **2009**, 3455; c) H. Fan, D. Adhikari, A. A. Saleh, R. L. Clark, F. J. Zuno-Cruz, G. Sanchez Cabrera, J. C. Huffman, M. Pink, D. J. Mindiola, M.-H. Baik, *J. Am. Chem. Soc.* **2008**, *130*, 17351; d) A. Jana, S. P. Sarish, H. W. Roesky, C. Schulzke, A. Döring, M. John, *Organometallics* **2009**, *28*, 2563.

[3] a) S. Pfirrmann, C. Limberg, C. Herwig, R. Stößer, B. Ziemer, *Angew. Chem.* **2009**, *121*, 3407; *Angew. Chem. Int. Ed.* **2009**, *48*, 3357; b) M. J. Henderson, C. H. L. Kennard, C. L. Raston, G. Smith, *J. Chem. Soc. Chem. Commun.* **1990**, 1203; c) E. Kogut, H. L. Wiencko, L. Zhang, D. E. Cordeau, T. H. Warren, *J. Am. Chem. Soc.* **2005**, *127*, 11248; d) W. H. Monillas, G. P. A. Yap, L. A. MacAdams, K. H. Theopold, *J. Am. Chem. Soc.* **2007**, *129*, 8090; e) K. Ding, W. W. Brennessel, P. L. Holland, *J. Am. Chem. Soc.* **2009**, *131*, 10804.

[4] a) S. Yao, Y. Xiong, X. Zhang, M. Schlangen, H. Schwarz, C. Milsmann, M. Driess, *Angew. Chem.* **2009**, *121*, 4621; *Angew. Chem. Int. Ed.* **2009**, *48*, 4551; b) E. C. Y. Tam, N. C. Johnstone, L. Ferro, P. B. Hitchcock, J. R. Fulton, *Inorg. Chem.* **2009**, *48*, 8971.

[5] P. J. Chirik, K. Wieghardt, *Science* **2010**, *327*, 794.

[6] P. Chaudhuri, C. N. Verani, E. Bill, E. Bothe, T. Weyhermüller, K. Wieghardt, *J. Am. Chem. Soc.* **2001**, *123*, 2213.

[7] W. Kaim, B. Schwederski, *Coord. Chem. Rev.* **2010**, *254*, 1580.

[8] S. G. McGeachin, *Can. J. Chem.* **1968**, *46*, 1903.

[9] a) R. Knorr, A. Weiß, *Chem. Ber.* **1981**, *114*, 2104; b) R. Knorr, H. Hauer, A. Weiss, H. Polzer, F. Ruf, P. Löw, P. Dvortsak, P. Böhrer, *Inorg. Chem.* **2007**, *46*, 8379.

[10] CCDC 777910 (**1**) and 777911 (**2**) contain the supplementary crystallographic data for this paper. These data can be obtained free of charge from The Cambridge Crystallographic Data Centre via www.ccdc.cam.ac.uk/data_request/cif.

[11] a) N. B. Morozova, P. A. Stabnikov, I. A. Baidina, P. P. Semyannikov, S. V. Trubin, I. K. Igumenov, *J. Struct. Chem.* **2007**, *48*, 889; b) M. Dochnahl, K. Lohnwitz, J. W. Pissarek, M. Biyikal, S. R. Schulz, S. Schon, N. Meyer, P. W. Roesky, S. Blechert, *Chem. Eur. J.* **2007**, *13*, 6654; c) K. D. Franz, G. M. McLaughlin, R. L. Martin, G. B. Robertson, *Acta Crystallogr. Sect. B* **1982**, *38*, 2476.

[12] a) M. M. Khusniyarov, K. Harms, O. Burghaus, J. Sundermeyer, *Eur. J. Inorg. Chem.* **2006**, 2985; b) M. M. Khusniyarov, K. Harms, O. Burghaus, J. Sundermeyer, B. Sarkar, W. Kaim, J. van Slageren, C. Duboc, J. Fiedler, *Dalton Trans.* **2008**, 1355.

[13] a) K. Chlopek, E. Bothe, F. Neese, T. Weyhermüller, K. Wieghardt, *Inorg. Chem.* **2006**, *45*, 6298; b) S. Blanchard, F. Neese, E. Bothe, E. Bill, T. Weyhermüller, K. Wieghardt, *Inorg. Chem.* **2005**, *44*, 3636.

[14] M. M. Khusniyarov, T. Weyhermüller, E. Bill, K. Wieghardt, *J. Am. Chem. Soc.* **2009**, *131*, 1208.

[15] The axes were chosen such that they are coincident with the C_2 axes of the pseudo-D_2 symmetry of the complex.

[16] C. K. Jörgensen, *Oxidation Numbers and Oxidation States*, Springer, Heidelberg, **1969**.

[17] a) D. Herebian, K. E. Wieghardt, F. Neese, *J. Am. Chem. Soc.* **2003**, *125*, 10997; b) V. Bachler, G. Olbrich, F. Neese, K. Wieghardt, *Inorg. Chem.* **2002**, *41*, 4179.

[18] O. Carugo, K. Djinovic, M. Rizzi, C. B. Castellani, *J. Chem. Soc. Dalton Trans.* **1991**, 1551.

